EMBO reports

EMBO open

scientific report

Drosophila syndecan regulates tracheal cell migration by stabilizing Robo levels

Joachim G. Schulz[1,2,3], Helga Ceulemans[1,3], Emmanuel Caussinus[4], Maria F. Baietti[1,3], Markus Affolter[4], Bassem A. Hassan[2,3+] & Guido David[1,3++]

[1]Laboratory of Glycobiology and Developmental Genetics, [2]Laboratory of Neurogenetics, Flanders Institute for Biotechnology (VIB), [3]Department of Human Genetics, Center for Human Genetics, Katholieke Universiteit Leuven, Leuven, Belgium, and [4]Growth and Development, Biozentrum der Universität Basel, Basel, Switzerland

Here we identify a new role for Syndecan (Sdc), the only transmembrane heparan sulphate proteoglycan in *Drosophila*, in tracheal development. Sdc is required cell autonomously for efficient directed migration and fusion of dorsal branch cells, but not for dorsal branch formation *per se*. The cytoplasmic domain of Sdc is dispensable, indicating that Sdc does not transduce a signal by itself. Although the branch-specific phenotype of *sdc* mutants resembles those seen in the absence of Slit/Robo2 signalling, genetic interaction experiments indicate that Sdc also helps to suppress Slit/Robo2 signalling. We conclude that Sdc cell autonomously regulates Slit/Robo2 signalling in tracheal cells to guarantee ordered directional migration and branch fusion.

Keywords: cell migration; *Drosophila*; heparan sulphate; Robo; tracheal system

EMBO *reports* (2011) **12**, 1039–1046. doi:10.1038/embor.2011.153

INTRODUCTION

Directed cell migration is a core mechanism in the establishment of branched organs such as the vasculature or the *Drosophila* tracheal system (Affolter *et al*, 2009). In both vertebrates and invertebrates, induction and guidance of cell migration towards a target are achieved by the coordinated action of several growth factor signalling pathways. One of the main questions is how these signalling pathways are coordinated and translated into highly stereotypic movements of small groups of cells (Ghabrial *et al*, 2003; Uv *et al*, 2003; Affolter & Caussinus, 2008; Lu & Werb, 2008; De Smet *et al*, 2009; Phng & Gerhardt, 2009).

[1]Laboratory of Glycobiology and Developmental Genetics,
[2]Laboratory of Neurogenetics, Flanders Institute for Biotechnology (VIB), and
[3]Department of Human Genetics, Center for Human Genetics, Katholieke Universiteit Leuven, Herestraat 49 bus 602, KU Leuven, Leuven 3000, Belgium
[4]Growth and Development, Biozentrum der Universität Basel, Basel 4056, Switzerland
[+]Corresponding author. Tel: +32 16 346218; Fax: +32 16 346226;
E-mail: bassem.hassan@cme.vib-kuleuven.be
[++]Corresponding author. Tel: +32 16 345863; Fax: +32 16 347166;
E-mail: guido.david@cme.vib-kuleuven.be

Received 9 November 2010; revised 14 June 2011; accepted 27 June 2011; published online 12 August 2011

Heparan sulphate, a glycosaminoglycan with highly complex structure, is essential for development, as the knockout of one of the enzymes essential for heparan sulphate synthesis is lethal early in development (Lin *et al*, 2000). We set out to investigate the function of the sole transmembrane heparan sulphate proteoglycan, Syndecan (Sdc), in *Drosophila* (Spring *et al*, 1994). Our data show for the first time, to our knowledge, that Sdc is required in tracheal morphogenesis. Sdc is crucial for fine-tuning of guided migration of the subset of epithelial cells constituting the tracheal dorsal branches. Sdc stabilizes Slit/Robo signalling and functions independently of its cytoplasmic domain.

RESULTS AND DISCUSSION

The *Syndecan* gene

The genome of *Drosophila melanogaster* harbours a single *sdc* gene. Existing mutants sdc^{23}, sdc^{48} and sdc^{97} are derived from imprecise P-element excisions causing deletions including *sdc* exons 1 and 2 (Fig 1A; Johnson *et al*, 2004; Steigemann *et al*, 2004), but these mutants all potentially affect the function of *Smad anchor for receptor activation* (*sara*) on the complementary strand (Epstein *et al*, 2002). We used ends-in homologous recombination (Rong *et al*, 2002) to introduce a frameshift mutation in exon 3 of *sdc* (Fig 1B). One line (sdc^{2639}) bearing the exon 3 mutation was further validated by genomic PCR, reverse transcription–PCR, western blotting (Fig 1C,D) and complementation analysis (Table 1). sdc^{2639} was semilethal in homozygosity and in trans-heterozygosity with sdc^{23}, sdc^{97}, sdc^{48} or the larger deficiencies Df^{PK1} or $Df^{exel6076}$. Similarly, the five other *sdc* exon 3 allele carrying stocks that we established were semilethal in trans-heterozygosity with sdc^{2639} or Df^{PK1}, but not over the deficiencies Df^{PI12} or Df^{XE2900}, which lie outside the *sdc* locus.

Syndecan tracheal branch phenotype

The external morphology of adult escaper sdc^{2639} flies had no obvious phenotype (not shown). However, inspection of *sdc* mutant third-instar larvae showed that the 10 dorsal branches of the tracheal system often failed to establish a dorsal anastomosis at the midline (Fig 2A–C), and ganglionic branch number and length were reduced (supplementary Fig S1). Dorsal branch fusion

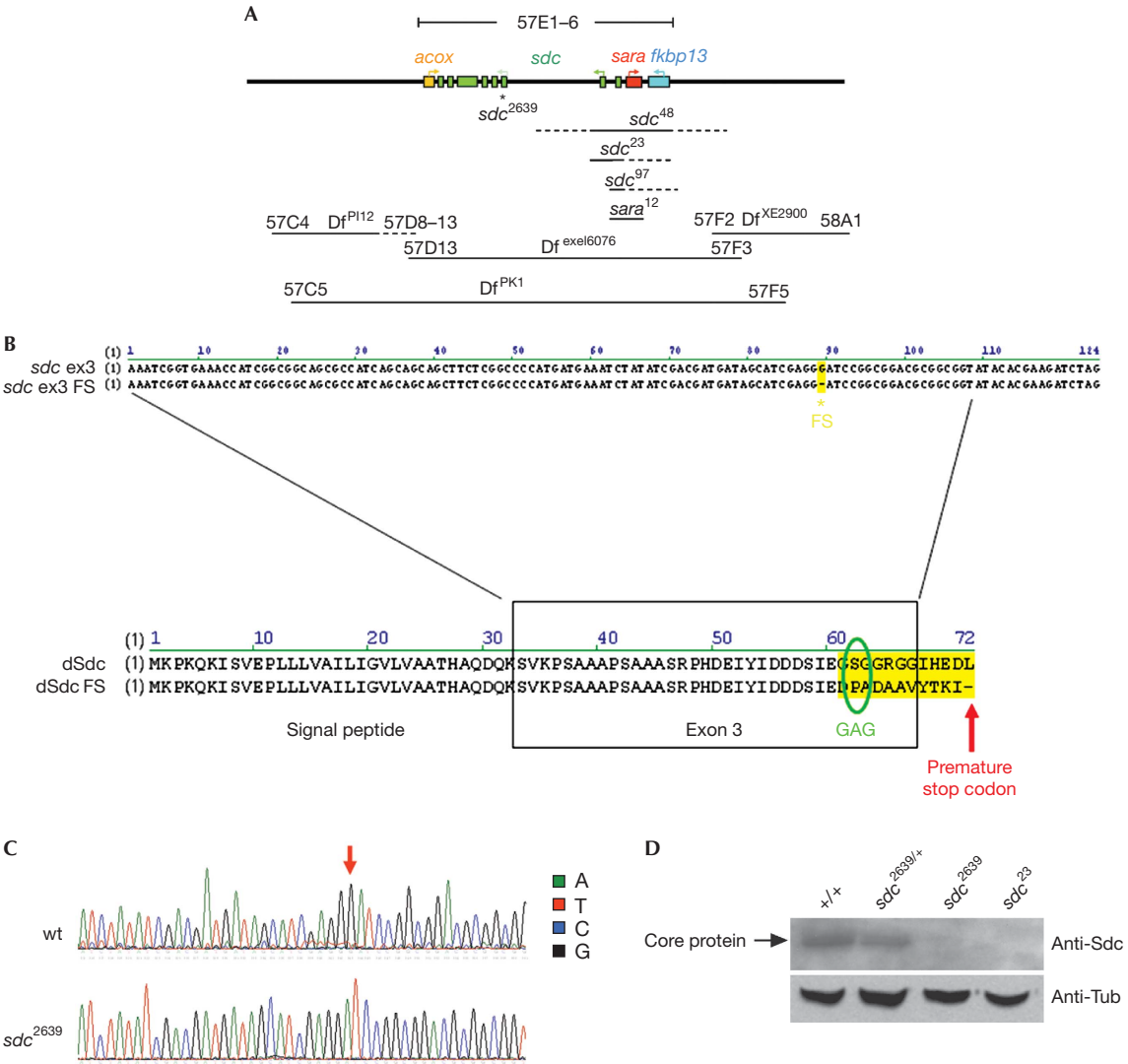

Table 1 | Complementation analysis of the *Syndecan* locus 57E2–6

Percentage of predicted eclosions	Df^{XE2900} 57F2–58A1	Df^{PI12} 57C4–57D13	$Df^{exel6076}$ 57D13–57F3	Df^{PK1} 57C5–57F5	*sdc*^{23}	*sdc*^{97}	*sdc*^{48}	*sdc*^{48}, *ubi*>*sara*	*sdc*^{2639}
$Df^{exel6076}$	71	107	0	1	40	47	0	0	29
sdc^{23}	109	88	40	23	9	30	35	48	51
sdc^{97}	104	114	35	14	30	20	39	50	32
sdc^{48}, *ubi*>*sara*	108	77	0	0	48	50	0	0	40
sdc^{2639}	96	118	29	30	51	32	41	40	26
sdc^{2451}	–	–	–	16	–	–	–	–	27
sdc^{2523}	–	–	–	20	–	–	–	–	24
sdc^{2527}	–	–	–	16	–	–	–	–	23
sdc^{2622}	–	–	–	26	–	–	–	–	15
sdc^{2626}	–	–	–	22	–	–	–	–	38
sdc^{2639}, *btl*>*sdc*	–	–	–	–	–	–	–	–	25

sara, Smad anchor for receptor activation; *sdc*, Syndecan.

Fig 1 | The *Syndecan* (*sdc*) gene and mutants. (**A**) Deficiencies and mutants spanning the *sdc* locus. The *sdc* locus on chromosome 2R. *sdc* (green) is flanked by *acox* (yellow) and *sara* (red) on the plus strand and *fkbp13* (blue) on the minus strand. sdc^{23} and sdc^{48} delete *sdc* exons 1 and 2, sdc^{97} deletes *sdc* exon 1, but they are not defined towards *sara*. $Df^{exel6076}$ and Df^{PK1} span the *sdc* locus, Df^{PI12} and Df^{XE2900} are outside the *sdc* locus. (**B**) *sdc* exon 3 sequence. Alignment of wild-type (upper) and *sdc* exon 3 mutant (lower) sequences. Upper alignment: Wild-type and mutant DNA sequences, with or without deletion of a guanidine residue in exon 3 that gives rise to a frameshift (FS). Lower alignment: Corresponding Sdc translation products with and without the premature stop codon with the new protein sequence after the frameshift (yellow), the first glycosaminoglycan (GAG) attachment site (green). (**C**) sdc^{2639} exon 3 RNA sequence. ABI sequencing of reverse-transcribed RNA of wild-type and *sdc* exon 3 mutant line sdc^{2639}. Red arrow, guanidine deleted in the mutant. (**D**) Effect of *sdc* mutants on Sdc protein level. Sdc protein levels in wild-type, $sdc^{2639}/+$, sdc^{2639} and sdc^{23} flies, on anti-Sdc western blot, anti-tubulin as loading control. Sdc, Syndecan; Tub, tubulin; wt, wild type.

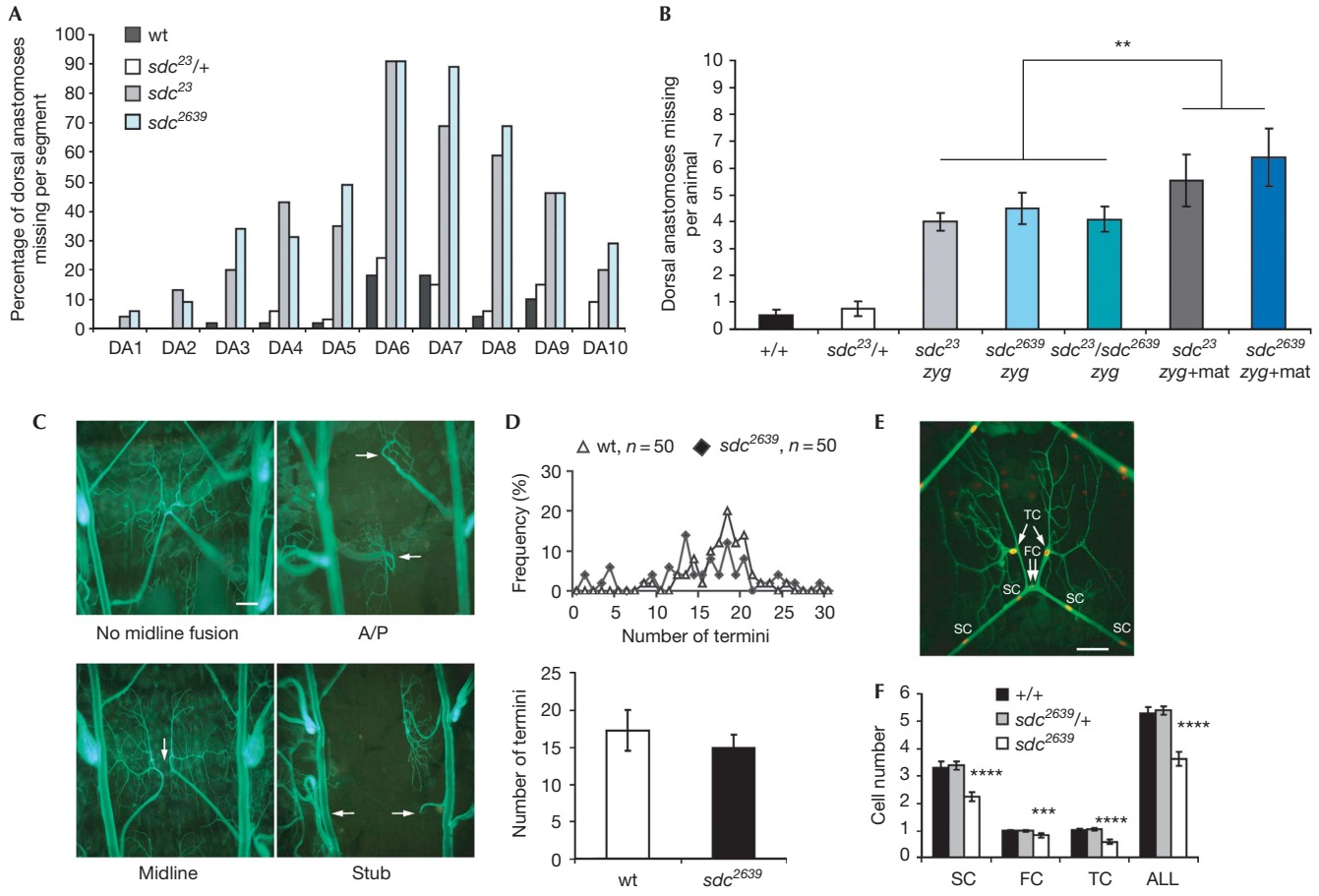

Fig 2 | *Syndecan* tracheal dorsal branch phenotype. (**A**) Segmental quantification of dorsal branch (DB) fusion failures in *sdc* mutants. Dorsal anastomoses (DA) missing in each of the 10 segments separately in wild-type (wt, black bar), sdc^{23} heterozygotes (white bar), sdc^{23} homozygotes (grey bar) or sdc^{2639} homozygotes (blue bar; $n \geqslant 35$ animals per genotype). (**B**) Quantification of total dorsal branch fusion failures in *sdc* mutants. The number of DA missing per animal, in wild type (black bar), $sdc^{23}/+$ (white bar), sdc^{23} from $sdc^{23}/+$ parents ('$sdc^{23}zyg$', light grey bar), sdc^{2639} from $sdc^{2639}/+$ parents ('$sdc^{2639}zyg$', light blue bar), sdc^{23}/sdc^{2639} from $sdc/+$ parents ('$sdc^{23}/sdc^{2639}zyg$', green bar), sdc^{23} from sdc^{23} parents ('$sdc^{23}zyg+$mat', dark grey bar), sdc^{2639} from sdc^{2639} parents ('sdc^{2639} $zyg+$mat', dark blue bar; ± confidence interval (CI), $n \geqslant 10$ animals per genotype; $^{**}P<0.01$ in *T*-test). (**C**) *sdc* dorsal branch phenotypes. Fluorescence stereomicroscopy of living sdc^{2639} third-instar larval filets expressing a tracheal CD8:GFP reporter to illustrate the categories of dorsal branch phenotypes. A/P, anterior–posterior misalignment; Stub, incomplete or absent branch. The arrows indicate the exact site of the phenotype. Scale bar, 100 μm. (**D**) Effect of *sdc* on dorsal branch terminal extension number. Upper: Frequency distribution for the number of termini ($n = 50$ cells) of wild-type (wt, open triangles) and sdc^{2639} (filled diamonds) terminal cells of the dorsal branch in segment 5 (DB5). Lower: Quantification of the average number of termini of wild-type (wt) and sdc^{2639} terminal cells in segment 5 (± CI; $n = 50$ cells). (**E**) Dorsal branch cell reporter. Fluorescence stereomicroscopy of two fused wild-type dorsal branches in a living third-instar larval filet expressing tracheal CD8:GFP and histone:RFP to label tracheal membranes and nuclei. Scale bar, 100 μm. (**F**) *sdc* dorsal branch cell numbers. Quantification of the number of dorsal branch cell types, in wild-type, $sdc^{2639}/+$ or sdc^{2639} larvae. FC, fusion cell; GFP, green fluorescent protein; RFP, red fluorescent protein; SC, stalk cell; TC, terminal cell (± CI; $^{***}P<0.005$; $^{****}P<0.001$ in *T*-test, $n = 30$ branches).

Table 2|Quantification of *Syndecan* dorsal branch cell types

Total	Stalk cells	Fusion cells	Terminal cells
6	4.0	1.0	1.0
5	3.07	0.97	0.97
4	2.13	1.05	0.82
3	1.83	0.93	0.23
2	1.81	0.19	0
1	0.83	0.17	0
0	0	0	0

Average contribution of stalk cells, fusion cells and terminal cells to *sdc* dorsal branch with a total cell number between 0 and 6 ($n = 30$ branches); *sdc*, *Syndecan*.

failures were observed only rarely in wild-type (0.5 non-fused segments per animal) or *sdc* heterozygotes (0.8 per animal; Fig 2A). By contrast, almost every second dorsal anastomosis was missing in sdc^{23} and sdc^{2639} mutants, in all segments at much higher rates but with a similar anterior–posterior distribution. In the progeny of escaper *sdc* mutant parents, which lack maternal and zygotic Sdc ('$sdc^{zyg+mat\prime}$), dorsal branch fusion failure rates were further elevated (5.6–6.4 per animal, Fig 2B) when compared with the zygotic mutants, whereas the dorsal trunk remained fused and primary branches were present. This result indicates that *sdc* has a branch-specific and incompletely penetrant role in tracheal development, a process that has many similarities with vertebrate angiogenesis, of which Sdc is a well-known modulator (Chen *et al*, 2004; Dedkov *et al*, 2007; Beauvais *et al*, 2009).

Syndecan cellular phenotypes

When a wild-type dorsal branch develops, 5–6 cells of the tracheal placode migrate dorsally and eventually intercalate. One of the tip cells develops into the terminal cell and extends fine terminal extensions, whereas the other tip cell becomes the fusion cell and forms a cell–cell contact with the fusion cell of the contralateral dorsal branch (Samakovlis *et al*, 1996; Tanaka-Matakatsu *et al*, 1996).

To understand the cellular mechanisms through which *sdc* affects dorsal branch fusion, we analysed the *sdc* dorsal branch phenotype at the single-cell level. We identified three dorsal branch phenotypes leading to fusion failures: dorsal branch that fail to meet at the midline because of anterior–posterior axis guidance defects ('A/P' phenotype), dorsal branch that reach the midline but fail to establish a dorsal anastomosis ('midline' phenotype), and, the most severe, incomplete dorsal branch or completely absent dorsal branch ('stub' phenotype; Fig 2C).

Although the terminal extensions were not significantly reduced in sdc^{2639} in segments in which terminal cells were found (Fig 2D), the average total number of dorsal branch cells was reduced from 5.3 or 5.4 cells in wild-type or heterozygous branches, respectively, to 3.6 cells in *sdc* mutant dorsal branches, affecting all three individual cell types: stalk cell (SC), terminal cell (TC) and fusion cell (FC; Fig 2E,F). Intriguingly, the loss of the different cell types was not random but followed a hierarchical order (Table 2). As the cells in a mature dorsal branch are arranged linearly, and their physical order from tip to base (TC/FC > SC > SC > SC > SC) is different from the hierarchical order we found for cell loss in *sdc* dorsal branch (SC > SC > TC > FC > SC > SC), cells cannot simply be lost from the end of the branch. More likely, Sdc is required for dorsal branch cell migration before cell intercalation and linear alignment, and before specification, which is known to occur after the cells leave the dorsal trunk (Ghabrial & Krasnow, 2006). Live imaging showed that many mechanisms accounted for a loss of *sdc* dorsal branch cells: an insufficient number of cells leaving the dorsal trunk (supplementary Video 1 online), reintegration of cells into the dorsal trunk (supplementary Video 2 online) and loss of cells from the branch (supplementary Video 3 online).

Syndecan cell autonomy

To test whether Sdc is required in a tissue-autonomous manner, we established Sdc Upstream Activating Sequence (UAS) knockdown lines (supplementary Fig S2 online). Dorsal branch fusion rates in pan-tracheal Sdc knockdown animals were similar to those observed in *sdc* mutants (Fig 3A compared with Fig 2A), and were completely reversed using an RNA interference-rescue '$sdc^{RESC\prime}$' transgene (Schulz *et al*, 2009; Fig 3A). Fusion-cell-specific Sdc knockdown was sufficient to induce dorsal branch fusion failures, and was also rescued with sdc^{RESC} (Fig 3B). We investigated whether Sdc expressed in only one fusion cell was sufficient for efficient dorsal branch fusion. We found that dorsal branch fusion still occurred in 15 out of 16 unilateral *sdc* fusion cell MARCM (mosaic analysis with a repressible cell marker) clones (Lee & Luo, 1999; Fig 3C, Table 3), indicating that Sdc might also function *in trans* on the contralateral fusion cell. Confocal images of stage 14 embryos of the Sdc-GFP FlyTrap line CC00871, which bears an in-frame, oriented green fluorescent protein (GFP) between Sdc exons 2 and 3, showed that Sdc is indeed expressed in developing dorsal branches (supplementary Fig S3A and B online).

Syndecan core protein function

Sdc is a type-I transmembrane protein with glycosaminoglycan chains attached to the ectodomain. Our RNAi Escape Strategy Construct (RESC) rescue approach allowed us to perform Sdc structure–function analyses in Sdc tracheal knockdown animals in surrounding wild-type tissue. The dorsal branch phenotype was completely reversed by wild-type Sdc, and also by a truncated version of Sdc lacking the cytoplasmic domain entirely ($Sdc^{\Delta C}$). Tracheal expression of Sdc did not rescue the semilethality observed in the mutant (Table 1), indicating that the tracheal phenotype alone does not account for lethality and that the tracheal Sdc is not sufficient for full viability. Sdc ectodomain alone (Sdc^{Ecto}) was partly functional in dorsal branch formation. Exon 5, coding for a large ectodomain sequence lacking in Sdc isoform B/C, was not essential in the context of dorsal branch fusion. By contrast, the Sdc core protein lacking glycosaminoglycan chains ($Sdc^{\Delta GAG}$) did not rescue tracheal dorsal branch fusion (Fig 3D). Wild-type Sdc or $Sdc^{\Delta C}$ expressed in tracheae fully rescued the dorsal branch phenotype in a *sdc* mutant background (Fig 3E). In summary, the glycosaminoglycan bearing ectodomain but not the cytoplasmic domain is essential for Sdc function, which is in line with the findings of Chanana *et al* (2009) in the nervous system.

Syndecan and Slit/Robo signalling

The combined dorsal branch and ganglionic branch phenotype we observed in *sdc* mutants and under tracheal knockdown

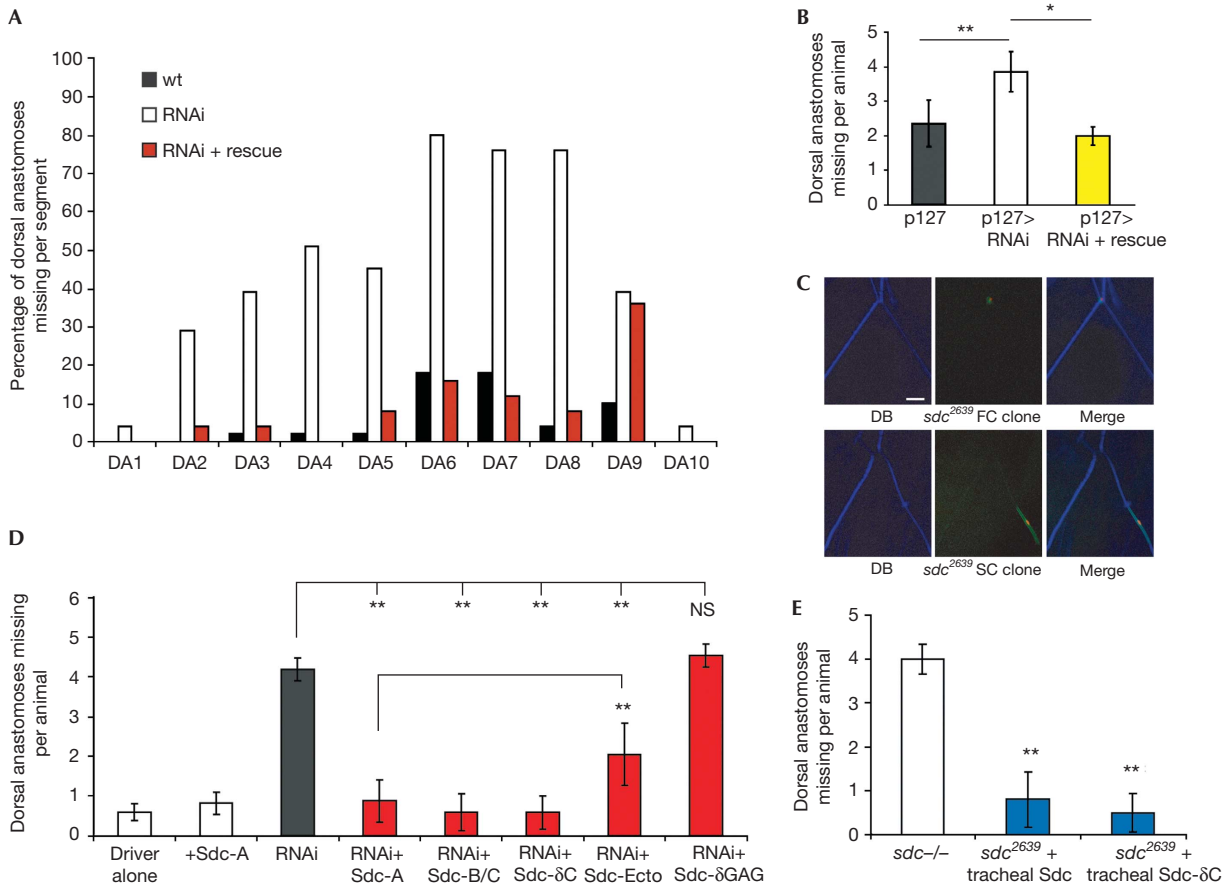

Fig 3 | Autonomy and rescue of *sdc* dorsal branch phenotype. (**A**) Quantification of dorsal branch fusion failures with Syndecan (Sdc) RNA interference (RNAi) and rescue. Dorsal anastomoses (DA) missing in each of the 10 segments, in wild-type (wt, black bars), btl > Gal4$^{3-1}$-driven tracheal Sdc RNAi alone (white bars) or tracheal Sdc knockdown with tracheal Sdc^{RESC} protein wt rescue (red bars; $n \geqslant 25$ animals/genotype). (**B**) Fusion-cell-specific Sdc RNAi and rescue. Quantification of total DA missing per third-instar larva expressing the fusion cell-specific driver p127 > Gal4 alone ('p127', black bar), with Sdc RNAi ('p127 > RNAi', white bar) or with Sdc RNAi and Sdc^{RESC} rescue ('p127 > RNAi + rescue', yellow bar; ± confidence interval (CI); $^{*}P < 0.05$; $^{**}P < 0.01$ in *T*-test, $n \geqslant 25$). (**C**) Dorsal branch with *sdc^{2639}* MARCM (mosaic analysis with a repressible cell marker) clone. Fluorescence stereomicroscopy of a third-instar *sdc^{2639}* fusion cell (upper panel) or stalk cell (lower panel) hs-Flippase (FLP)-induced clone, positively marked with CD8:GFP, histone:RFP (MARCM technique) and btl-Gal4$^{3-1}$. Scale bar, 100 μm. (**D**) Rescue of tracheal Sdc RNAi with Sdc protein mutants. DA missing per animal with tracheal driver btl-Gal4$^{3-1}$ alone (white bar), tracheal overexpression of long Sdc isoform A ('Sdc-A', white bar), tracheal Sdc knockdown alone ('RNAi', black bar) or tracheal Sdc knockdown with Sdc RESC rescue construct (red bars) bearing protein wild-type Sdc-A^{RESC} ('RNAi + Sdc-A'), protein wild-type Sdc-B/C lacking exon 5 coding for part of the extracellular domain ('RNAi + Sdc-B/C'), Sdc^{RESC} lacking the cytoplasmic domain ('RNAi + Sdc-δC'), Sdc^{RESC} ectodomain ('RNAi + Sdc-Ecto') or Sdc^{RESC} lacking the glycosaminoglycan-attachment sites ('RNAi + Sdc–δGAG'; ± CI; $^{**}P < 0.01$ in *T*-test, $n \geqslant 10$ animals per genotype). (**E**) Rescue of *sdc* mutant dorsal branch phenotype. Dorsal branch missing per animal in *sdc^{2639}* (white), *sdc^{2639}* with tracheal protein wild-type Sdc ('tracheal Sdc') or Sdc lacking the cytoplasmic domain ('tracheal Sdc-δC) rescue (blue; ± CI; $^{*}P < 0.05$; $^{**}P < 0.01$ in *T*-test, $n \geqslant 10$). GFP, green fluorescent protein; NS, non-significant.

Table 3 | *Syndecan* dorsal branch MARCM clones

Cell type	Number of clones	Percentage of clones	Number of clones in non-fused dorsal branch	Percentage of clones in non-fused dorsal branch
Stalk cell	47	74.6	4	8.5
Fusion cell	16	25.4	1	6.3
Terminal cell	0	0	0	NA
Total	63	100	5	7.9

Clones are generated by hs > FLP-induced recombination and positively marked with GFP and RFP (MARCM technique). Indicated are the absolute number or the percentage of clones found in one of the three dorsal branch cell types, and whether these clones are part of a fused or non-fused branch. DB, dorsal branch; GFP, green fluorescent protein; MARCM, mosaic analysis with a repressible cell marker; NA, not applicable; *sdc*, *Syndecan*.

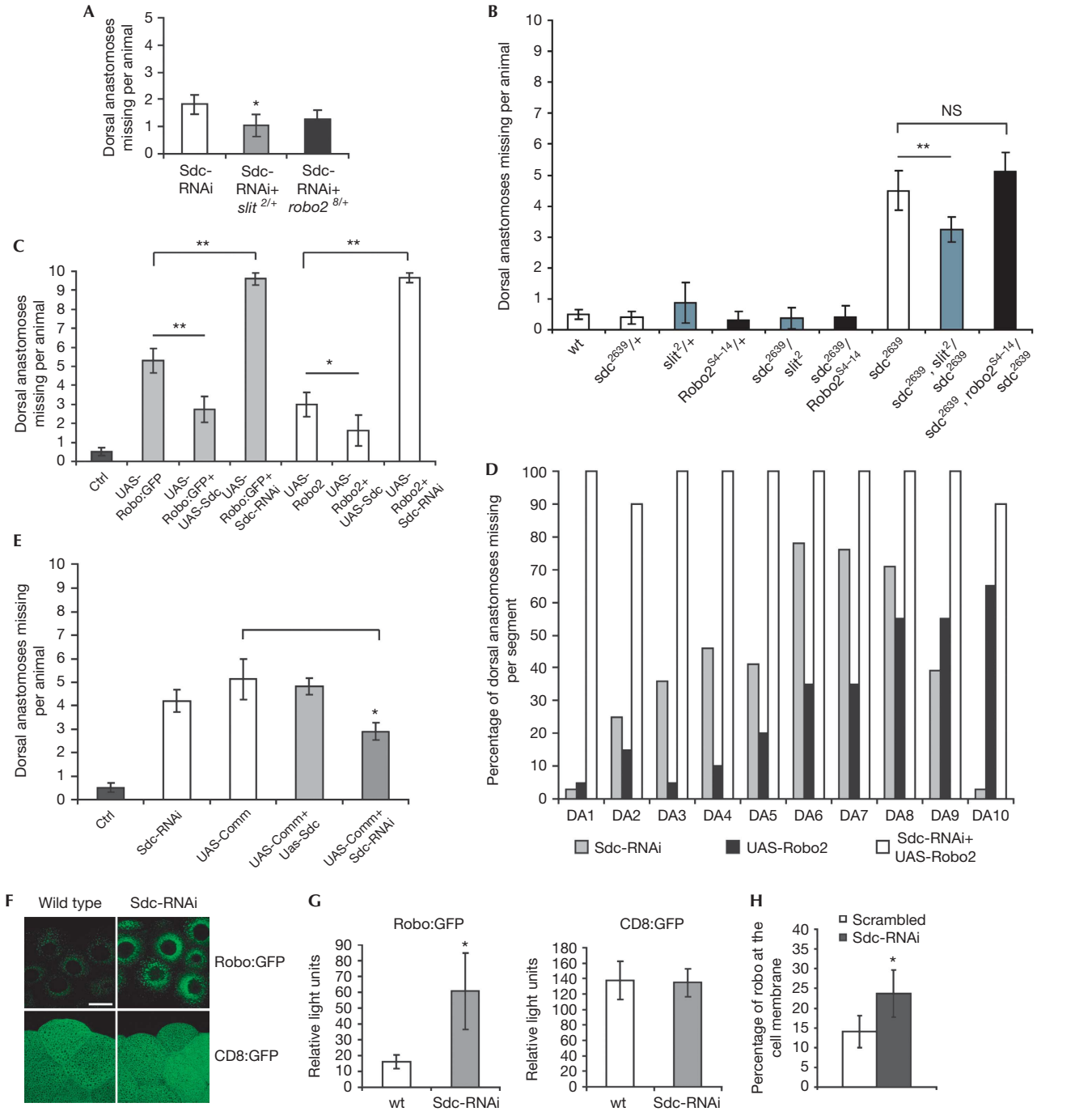

conditions was highly reminiscent of the phenotype observed in *slit* or *robo2* mutants (Englund *et al*, 2002). Therefore, we proposed that *sdc* interacts with *slit/robo2* in tracheal development. To test this prediction, we combined an intermediate Sdc knockdown with a loss-of-function *slit* or *robo2* allele in heterozygosity (Fig 4A). The *sdc* dorsal branch phenotype was suppressed by heterozygosity for the ligand *slit*. Heterozygous loss of the receptor *robo2* had a smaller effect, not reaching statistical significance (Fig 4A). Heterozygosity for *slit* in a homozygous *sdc* mutant suppressed the dorsal branch phenotype as well, whereas neither *sdc* and *slit* or *sdc* and *robo2* in transheterozygosity, nor a heterozygous *robo2* allele in combination with an *sdc* mutant had an effect (Fig 4B). This indicates that the *sdc* loss-of-function phenotype is due to a gain in Slit/Robo2 signalling that is more sensitive to *slit* than to *robo2* heterozygosity. In agreement with this hypothesis, tracheal Robo or Robo2 overexpression alone caused a dorsal branch fusion phenotype, Sdc overexpression suppressed the Robo overexpression phenotype and Sdc knockdown markedly enhanced the Robo overexpression phenotype (Fig 4C,D). Moreover, tracheal overexpression of Commissureless,

◀ **Fig 4** | *Syndecan* and Slit/Robo signalling. (**A**) Genetic interaction of *Syndecan* (*sdc*) and *slit* or *robo2*. Dorsal anastomoses (DA) missing per animal, in intermediate (btl > Gal4[1] at 25 °C, white bar) tracheal Sdc knockdown alone ('Sdc-RNAi', white bar) or with one copy of a *slit* ('Sdc-RNAi + *slit*^{2}/+', grey bar) or *robo2* allele ('Sdc-RNAi + *robo2*^{8}/+', black bar; ± confidence interval (CI); **P* < 0.05 in *T*-test, *n* = 30 per genotype). (**B**) Genetic interaction of *sdc* and *slit* or *robo2*. DA missing per animal, in wild type (wt), heterozygotes (*sdc*^{2639}/+, *slit*^{2}/+ *or robo2*$^{S4-14}$/+), transheterozygotes (*sdc*^{2639}/*slit*^{2} *or sdc*^{2639}/*robo2*$^{S4-14}$) *or sdc* zygotic mutant in combination with one copy of a *slit* (*sdc*^{2639},*slit*^{2}/*sdc*^{2639}) or a *robo2* (*sdc*^{2639},*robo2*$^{S4-14}$/*sdc*^{2639}) allele (± CI; *n* ⩾ 10 animals per genotype; ***P* < 0.01 in *T*-test). (**C**) Genetic interaction of *sdc* and *robo* or *robo2*. DA missing per animal in control ('Ctrl', black bar), btl > Gal4$^{3-1}$-induced tracheal overexpression of Robo ('UAS-Robo:GFP', grey bars), or Robo2 ('UAS-Robo2', white bars) alone, or in combination with overexpression ('UAS-Sdc'), or knockdown ('Sdc-RNAi') of Sdc (± CI; **P* < 0.05; ***P* < 0.01 in *T*-test, *n* ⩾ 10 per genotype). (**D**) Genetic interaction of *sdc* and *robo2*. DA missing per segment, in btl > Gal4$^{3-1}$-induced tracheal Sdc knockdown alone ('Sdc-RNAi', grey bars), Robo2 overexpression alone ('UAS-robo2', yellow bars) or both ('Sdc-RNAi + UAS-robo2', white bars; *n* = 30 per genotype). (**E**) Genetic interaction of *sdc* and *comm*. DA missing per animal, in control ('ctrl', black bar); btl > Gal4$^{3-1}$-induced tracheal Sdc knockdown ('Sdc-RNAi', white bar), tracheal Comm overexpression ('UAS-comm', white bar), Comm and Sdc overexpression ('UAS-comm + UAS-Sdc', light grey bar) or Comm overexpression and Sdc knockdown ('UAS-comm + Sdc-RNAi', dark grey bar; ± CI; ***P* < 0.01 in *T*-test, *n* = 30 per genotype). (**F**) Influence of Sdc on Robo:GFP or CD8:GFP levels. Confocal images of third-instar larval salivary glands expressing Robo:GFP or CD8:GFP with fkh > Gal4, in the presence or absence of Sdc-RNAi. (**G**) Influence of Sdc on Robo:GFP or CD8:GFP levels. Quantification fkh > Gal4-driven Robo2:GFP or CD8:GFP signal intensity in third-instar larval salivary glands, in the presence or absence of Sdc-RNAi (± CI; ***P* < 0.01 in *T*-test, *n* = 10 per genotype). (**H**) Effect of Sdc on endogenous Robo levels. Cell membrane Robo1 levels in human MCF7 cells treated with non-targeting (scrambled) or Sdc1/Sdc4-targeting small interfering RNA (expressed as a percentage of total Robo1, ± CI; **P* < 0.05 in *T*-test, *n* = 3). Comm, Commissureless; GFP, green fluorescent protein; NA, non-significant; RNAi, RNA interference.

known to downregulate Robo in axons committed to cross the midline (Keleman *et al*, 2002, 2005; Myat *et al*, 2002), resulted in a dorsal branch fusion phenotype that was significantly attenuated by Sdc knockdown (Fig 4E).

As Sdc functions cell autonomously (Fig 3), it might suppress Slit/Robo signalling by affecting Robo levels. When we performed Robo stainings of stage 13/14 wild-type, *sdc* mutant, or tracheal Sdc overexpressing embryos, we could not detect a change in Robo2 or Robo signal intensity (supplementary Fig S4A,B online). As this might be due to the dynamic expression of Robo or to a lack of sensitivity of the staining method, we addressed this further in systems in which Robo levels are more quantifiable. In salivary glands, Sdc knockdown caused a 3.7-fold increase in ectopically expressed Robo:GFP levels, but not in the levels of a control transmembrane protein, CD8:GFP (Fig 4F,G). To confirm the effect of Sdc on endogenous Robo levels, we knocked down Sdc in human MCF7 cells, expressing Robo1, Sdc1 and Sdc4, and found a significant 1.8-fold increase in cell surface Robo localization (Fig 4H).

Our genetic interaction studies in combination with the cell culture experiments strongly indicate that disrupted Slit/Robo2 signalling accounts for the branch-specific and incompletely penetrant *sdc* tracheal phenotype (Englund *et al*, 2002). The insufficient restriction of Slit/Robo2 signalling in space and/or time in *sdc* mutants might generate aberrant attractive forces and disrupt spatial information. A general role for Sdc in Slit/Robo signalling is likely, as the different Robo receptors share the same extracellular domain structure.

In addition to the known role of Sdc in promoting Slit/Robo signalling, as shown for axon guidance in the nervous system (Johnson *et al*, 2004; Steigemann *et al*, 2004; Rhiner *et al*, 2005; Chanana *et al*, 2009), we now show that tracheal Sdc can also suppress Slit/Robo2 signalling. At present, such dual function is not explained, but a similar buffering role has been suggested for another heparan sulphate proteoglycan, Dally-like, in Wingless signalling (Kreuger *et al*, 2004). Whether signalling is enhanced or suppressed by Sdc might depend on Slit/Robo and Sdc levels, and also on the concomitant expression of other heparan sulphate proteoglycans. Alternatively, it could be related to the tissue-specific mode of action of Slit/Robo signalling, switching between attractive and repulsive depending on the tissue or the stage of development (Kramer *et al*, 2001; Englund *et al*, 2002).

How could Sdc function on Robo2 levels? We show that Sdc is required cell autonomously, in the same cells as Robo2 is expressed, and find that Sdc can downregulate Robo post-translationally. Sdc might be required for sorting a fraction of *de novo* synthesized Robo2 directly to a degradation pathway, similar to the function of Commissureless, transporting Robo directly from the synthetic pathway to late endosomes, thereby preventing Robo cell surface expression (Kidd *et al*, 1998; Keleman *et al*, 2005). Alternatively, Sdc might promote the removal of Robo2 from the cell surface or an endosomal recycling compartment, as Sdc is known to be important for endosomal growth factor receptor endocytosis and recycling (Tkachenko *et al*, 2004; Zimmermann *et al*, 2005). Interestingly, Arf6, a central component in epithelial cell migration and endosomal recycling (Palacios *et al*, 2001; Sabe, 2003), has been recently identified as a downstream target of Slit/Robo signalling in angiogenesis (Jones *et al*, 2009). Hence Sdc might regulate Robo transport to or from an Arf6 endosomal compartment.

In conclusion, we provide genetic, biochemical and cell biological evidence for a specific role for Sdc in tracheal development where cell autonomous Sdc is required for Slit/Robo2-mediated cell migration and midline fusion of the dorsal branch.

METHODS

For more details see supplementary information online.

Constructs. Sdc constructs were cloned into pUAST. The Sdc RNAi line target exons 6 and 7, and this sequence was replaced within the Sdc rescue lines by a RESC sequence.

Sdc$^{\Delta C}$ contains a stop codon after Lys 368, Sdc^{Ecto} a stop after Asn 318 and Sdc$^{\Delta GAG}$ Ser > Ala mutations of amino acids 62, 79, 81, 110 and 194. The *sdc* homologous recombination mutant contains a deletion of guanine at position 89 of exon 3, producing a premature stop codon.

Standard culture conditions. Flies were maintained on standard fly food at 25 °C. RNAi experiments were conducted at 28 °C except when indicated differently.

Supplementary information is available at EMBO *reports* online (http://www.emboreports.org).

ACKNOWLEDGEMENTS

We thank J. Lincecum (Boston) for providing *sdc* complementary DNA and antibody, and D. Smith (University of Texas, Dallas), G. Vorbrüggen (MPI Göttingen), G. Struhl (Columbia University), M. Krasnow (Stanford University), B. Dickson (IMP Wien), S. Selleck (University of Minnesota), J. Knoblich (IMBA Wien), M. Llimargas (IBMB Barcelona), A. Spradling (Flytrap), the Bloomington Drosophila Stock Center (University of Indiana) and R. Ueda (National Institute of Genetics, Shizuoka) for providing fly stocks. This work was supported by grants from the National Fund for Scientific Research – Flanders (FWO) to G.D. and B.A.H.; Flanders Institute for Biotechnology (VIB) to G.D. and B.A.H.; Interuniversity Attraction Poles Program of the Belgian Federal Government to G.D.; and K.U. Leuven to G.D. (GOA) and B.A.H. (Impuls, CREA, GOA), a FEBS fellowship and an EMBO long-term postdoctoral fellowship to E.C., and grants from the Kantons Basel-Stadt and Basel-Land, from the Swiss National Science Foundation and a Network of Excellence grant 'Cells into Organs' from the Framework Program 6 of the European Community to the laboratory of M.A.

CONFLICT OF INTEREST

The authors declare that they have no conflict of interest.

REFERENCES

Affolter M, Caussinus E (2008) Tracheal branching morphogenesis in *Drosophila*: new insights into cell behaviour and organ architecture. *Development* **135:** 2055–2064

Affolter M, Zeller R, Caussinus E (2009) Tissue remodelling through branching morphogenesis. *Nat Rev Mol Cell Biol* **10:** 831–842

Beauvais DM, Ell BJ, McWhorter AR, Rapraeger AC (2009) Syndecan-1 regulates alphavbeta3 and alphavbeta5 integrin activation during angiogenesis and is blocked by synstatin, a novel peptide inhibitor. *J Exp Med* **206:** 691–705

Chanana B, Steigemann P, Jackle H, Vorbruggen G (2009) Reception of Slit requires only the chondroitin-sulphate-modified extracellular domain of Syndecan at the target cell surface. *Proc Natl Acad Sci USA* **106:** 11984–11988

Chen E, Hermanson S, Ekker SC (2004) Syndecan-2 is essential for angiogenic sprouting during zebrafish development. *Blood* **103:** 1710–1719

De Smet F, Segura I, De Bock K, Hohensinner PJ, Carmeliet P (2009) Mechanisms of vessel branching: filopodia on endothelial tip cells lead the way. *Arterioscler Thromb Vasc Biol* **29:** 639–649

Dedkov EI, Thomas MT, Sonka M, Yang F, Chittenden TW, Rhodes JM, Simons M, Ritman EL, Tomanek RJ (2007) Synectin/syndecan-4 regulate coronary arteriolar growth during development. *Dev Dyn* **236:** 2004–2010

Englund C, Steneberg P, Falileeva L, Xylourgidis N, Samakovlis C (2002) Attractive and repulsive functions of Slit are mediated by different receptors in the *Drosophila* trachea. *Development* **129:** 4941–4951

Epstein EA, Martin JM, O'Connor MB (2002) Genetics of the sara and syndecan region. *A Dros Res Conf* **43:** 445A

Ghabrial A, Luschnig S, Metzstein MM, Krasnow MA (2003) Branching morphogenesis of the *Drosophila* tracheal system. *Annu Rev Cell Dev Biol* **19:** 623–647

Ghabrial AS, Krasnow MA (2006) Social interactions among epithelial cells during tracheal branching morphogenesis. *Nature* **441:** 746–749

Johnson KG, Ghose A, Epstein E, Lincecum J, O'Connor MB, Van Vactor D (2004) Axonal heparan sulfate proteoglycans regulate the distribution and efficiency of the repellent slit during midline axon guidance. *Curr Biol* **14:** 499–504

Jones CA *et al* (2009) Slit2-Robo4 signalling promotes vascular stability by blocking Arf6 activity. *Nat Cell Biol* **11:** 1325–1331

Keleman K, Rajagopalan S, Cleppien D, Teis D, Paiha K, Huber LA, Technau GM, Dickson BJ (2002) Comm sorts robo to control axon guidance at the *Drosophila* midline. *Cell* **110:** 415–427

Keleman K, Ribeiro C, Dickson BJ (2005) Comm function in commissural axon guidance: cell-autonomous sorting of Robo *in vivo*. *Nat Neurosci* **8:** 156–163

Kidd T, Russell C, Goodman CS, Tear G (1998) Dosage-sensitive and complementary functions of roundabout and commissureless control axon crossing of the CNS midline. *Neuron* **20:** 25–33

Kramer SG, Kidd T, Simpson JH, Goodman CS (2001) Switching repulsion to attraction: changing responses to slit during transition in mesoderm migration. *Science* **292:** 737–740

Kreuger J, Perez L, Giraldez AJ, Cohen SM (2004) Opposing activities of Dally-like glypican at high and low levels of Wingless morphogen activity. *Dev Cell* **7:** 503–512

Lee T, Luo L (1999) Mosaic analysis with a repressible cell marker for studies of gene function in neuronal morphogenesis. *Neuron* **22:** 451–461

Lin X, Wei G, Shi Z, Dryer L, Esko JD, Wells DE, Matzuk MM (2000) Disruption of gastrulation and heparan sulfate biosynthesis in EXT1-deficient mice. *Dev Biol* **224:** 299–311

Lu P, Werb Z (2008) Patterning mechanisms of branched organs. *Science* **322:** 1506–1509

Myat A, Henry P, McCabe V, Flintoft L, Rotin D, Tear G (2002) *Drosophila* Nedd4, a ubiquitin ligase, is recruited by Commissureless to control cell surface levels of the roundabout receptor. *Neuron* **35:** 447–459

Palacios F, Price L, Schweitzer J, Collard JG, D'Souza-Schorey C (2001) An essential role for ARF6-regulated membrane traffic in adherens junction turnover and epithelial cell migration. *EMBO J* **20:** 4973–4986

Phng LK, Gerhardt H (2009) Angiogenesis: a team effort coordinated by notch. *Dev Cell* **16:** 196–208

Rhiner C, Gysi S, Frohli E, Hengartner MO, Hajnal A (2005) Syndecan regulates cell migration axon guidance in *C. elegans*. *Development* **132:** 4621–4633

Rong YS, Titen SW, Xie HB, Golic MM, Bastiani M, Bandyopadhyay P, Olivera BM, Brodsky M, Rubin GM, Golic KG (2002) Targeted mutagenesis by homologous recombination in *D. melanogaster*. *Genes Dev* **16:** 1568–1581

Sabe H (2003) Requirement for Arf6 in cell adhesion, migration, and cancer cell invasion. *J Biochem* **134:** 485–489

Samakovlis C, Manning G, Steneberg P, Hacohen N, Cantera R, Krasnow MA (1996) Genetic control of epithelial tube fusion during *Drosophila* tracheal development. *Development* **122:** 3531–3536

Schulz JG, David G, Hassan BA (2009) A novel method for tissue-specific RNAi rescue in *Drosophila*. *Nucleic Acids Res* **37:** e93

Spring J, Paine-Saunders SE, Hynes RO, Bernfield M (1994) *Drosophila* syndecan: conservation of a cell-surface heparan sulfate proteoglycan. *Proc Natl Acad Sci USA* **91:** 3334–3338

Steigemann P, Molitor A, Fellert S, Jackle H, Vorbruggen G (2004) Heparan sulfate proteoglycan syndecan promotes axonal and myotube guidance by slit/robo signaling. *Curr Biol* **14:** 225–230

Tanaka-Matakatsu M, Uemura T, Oda H, Takeichi M, Hayashi S (1996) Cadherin-mediated cell adhesion and cell motility in *Drosophila* trachea regulated by the transcription factor Escargot. *Development* **122:** 3697–3705

Tkachenko E, Lutgens E, Stan RV, Simons M (2004) Fibroblast growth factor 2 endocytosis in endothelial cells proceed via syndecan-4-dependent activation of Rac1 and a Cdc42-dependent macropinocytic pathway. *J Cell Sci* **117:** 3189–3199

Uv A, Cantera R, Samakovlis C (2003) *Drosophila* tracheal morphogenesis: intricate cellular solutions to basic plumbing problems. *Trends Cell Biol* **13:** 301–309

Zimmermann P, Zhang Z, Degeest G, Mortier E, Leenaerts I, Coomans C, Schulz JG, N'Kuli F, Courtoy PJ, David G (2005) Syndecan recycling is controlled by syntenin-PIP2 interaction and Arf6. *Dev Cell* **9:** 377–388